

# Refusal-Feature-guided Teacher for Safe Finetuning via Data Filtering and Alignment Distillation

Seokil Ham   Yubin Choi   Seungju Cho   Yujin Yang   Younghun Kim   Changick Kim

Korea Advanced Institute of Science and Technology (KAIST)

Daejeon, South Korea

{gkatjrldf, choibinbin, joyga, ujin.y, younghun1664, changick}@kaist.ac.kr

## Abstract

Recently, major AI service providers such as Google and OpenAI have introduced Finetuning-as-a-Service, which enables users to customize Large Language Models (LLMs) for specific downstream tasks using their own data. However, this service is vulnerable to degradation of LLM safety-alignment when user data contains harmful prompts. While some prior works address this issue, fundamentally filtering harmful data from user data remains unexplored. Motivated by our observation that a directional representation reflecting refusal behavior (called the refusal feature) obtained from safety-aligned LLMs can inherently distinguish between harmful and harmless prompts, we propose the Refusal-Feature-guided Teacher (ReFT). Our ReFT model is trained to identify harmful prompts based on the similarity between input prompt features and its refusal feature. During finetuning, the ReFT model serves as a teacher that filters harmful prompts from user data and distills alignment knowledge into the base model. Extensive experiments demonstrate that our ReFT-based finetuning strategy effectively minimizes harmful outputs and enhances finetuning accuracy for user-specific tasks, offering a practical solution for secure and reliable deployment of LLMs in Finetuning-as-a-Service.

## 1 Introduction

Recent advancements in Large Language Models (LLMs) [1, 9, 18, 20, 35, 42, 43] have achieved remarkable performance across a broad range of natural language processing tasks, including commonsense reasoning, question answering, summarization, and dialogue generation. The LLMs are typically pretrained on vast and diverse corpora, resulting in strong generalization capabilities and allowing wide applicability across domains. To further facilitate LLMs for individual and domain-specific purposes, major AI service providers such as Google and OpenAI offer not only access to pretrained LLMs but also Finetuning-as-a-Service. This service enables users to upload custom datasets and adapt LLMs to more specific tasks and domains depending on their unique requirements.

However, finetuning services must safeguard against the malicious use of LLMs through safety-alignment, even when users attempt to jailbreak the models via customization. To mitigate these risks, Finetuning-as-a-Service typically adopts a two-stage pipeline. In the first stage, referred to as the alignment stage, pretrained LLMs are trained to avoid generating harmful responses to harmful prompts and to produce helpful responses to harmless prompts. In the second stage, referred to as the finetuning stage, the aligned models are finetuned on user data for customized downstream tasks. Despite this two-stage approach, several studies [10, 14, 15, 16, 22, 36] have shown that finetuning on user data containing harmful content can compromise the safety-alignment initially achieved during the alignment stage. These types of attacks, which inject harmful prompts into user data for

finetuning, are called harmful finetuning attacks. The presence of such attacks highlights the need to preserve model safety while achieving high performance on user tasks in Finetuning-as-a-Service.

To address the harmful finetuning attacks, prior works have proposed solutions that mainly target either alignment stage [15, 16, 36] or finetuning stage [14, 22, 23, 30]. However, our experimental results in Table 2 reveal that maintaining safety-alignment through alignment-stage solutions is challenging as the proportion of harmful prompts in user data increases. This vulnerability is particularly critical in adversarial scenarios, where malicious attackers aiming to jailbreak LLMs inject a large number of harmful prompts into user data to maximize the likelihood of a successful attack. In addition, although identifying and removing harmful prompts from user data is a fundamental approach for safe finetuning, methods for directly filtering harmful prompts remain largely underexplored.

Therefore, in this work, we propose a novel finetuning-stage solution that ensures safe finetuning by filtering harmful prompts from user data during finetuning. Motivated by our observations that the refusal feature obtained from safety-aligned LLMs can effectively distinguish between harmful and harmless prompts, we introduce Refusal-Feature-guided Teacher (ReFT) model. The ReFT model is designed not only to accurately classify prompts based on their harmfulness using its refusal feature, but also to generate appropriate refusal responses to harmful requests. During finetuning stage, the ReFT model is utilized as a teacher for two different purposes. First, the ReFT model serves as a teacher for **Data Filtering** by identifying and removing harmful prompts from user data based on its refusal features, thereby preventing safety-degradation caused by exposure to harmful data. Second, the ReFT model serves as a teacher model for **Alignment Distillation**, generating soft refusal labels that provide more informative supervision. These soft refusal labels guide the student model to follow the safety-aligned behavior of the ReFT model. Furthermore, the soft labels help smooth the alignment loss surface, allowing more seamless integration with the finetuning loss on user data.

Our extensive experimental results demonstrate the effectiveness of our ReFT-based finetuning strategy in both user-specific downstream task performance and safety-alignment. In most cases, our method achieves the highest finetuning accuracy and the lowest harmful score compared to our baselines. Consequently, incorporating ReFT-based harmful data filtering and alignment knowledge distillation provides a practical solution for the secure and reliable deployment of LLMs. Additionally, our observations offer a novel insight for future research: the refusal feature extracted from safety-aligned LLMs can be a reliable indicator for distinguishing between harmful and harmless data.

### Our Contributions

- To the best of our knowledge, this work presents the first analysis of refusal features in aligned LLMs for differentiating harmful and harmless prompts. Our observations suggest that refusal features can serve as strong indicators for accurately classifying the harmfulness of prompts.
- Based on our observations, we propose the ReFT model and a ReFT-based finetuning strategy that leverage the refusal feature of the ReFT model to enable both (i) accurate filtering of harmful prompts from user data and (ii) safety-alignment knowledge distillation during finetuning.
- Our experimental results demonstrate the effectiveness of harmful data filtering and alignment knowledge distillation based on the ReFT model, achieving strong performance on user-specific downstream tasks while consistently preserving model safety across diverse settings.

## 2 Related Works

**Safety in Large Language Models.** Large Language Models (LLMs) can respond to a wide range of user queries but are vulnerable to harmful prompts [19, 55], which induce harmful outputs such as instructions for making weapons or generating fake news content. To mitigate these risks, safety-aligned LLMs [1, 2, 42] have been introduced. These models are finetuned using Supervised FineTuning (SFT) [5] or Reinforcement Learning with Human Feedback (RLHF) [31, 34] on large-scale safety-alignment datasets that consist of harmful prompts paired with harmless (refusal) responses. As a result, safety-aligned models are capable of refusing harmful requests. However, safety-aligned models are still vulnerable to advanced jailbreaking techniques [6, 24, 27, 55]. Then, recent studies have focused on extensively enhancing the safety of LLMs, and existing approaches can be broadly categorized into training-free and training-based methods. Some training-free-based methods leverage the inherent capabilities of LLMs to assess harmfulness [44] or predict user intent [52]. Other methods exploit internal differences in the model, such as parameters [47], gradients [12], or attention patterns [17], when processing harmful versus harmless inputs. In contrast, training-based methods

aim to enhance robustness by finetuning LLMs through adversarial training or by training auxiliary models. Some adversarial training approaches investigate the balance between harmful and harmless prompts used during finetuning [5], or utilize adversarial samples generated by adding perturbations to the latent space [37, 38, 46, 54]. Other methods train separate safe and unsafe (auxiliary) models and apply safe decoding strategies [4, 8, 48, 53]. Recently, the concept of a refusal feature, which encodes the refusal behavior of safety-aligned LLMs, is introduced, leveraging it in both adversarial attacks [3] and defense [50]. Building on the insight of the refusal feature, we further analyze the refusal feature and demonstrate its effectiveness in classifying prompts as harmful or harmless. Based on the capability of refusal feature, we propose a novel finetuning strategy for safe LLM finetuning.

**Harmful Finetuning Attacks.** In addition to jailbreaking attacks that induce harmful responses through input prompts, harmful finetuning attacks also pose a significant threat to the safety of LLMs by compromising the safety during finetuning. These attacks are a subclass of jailbreaking techniques in which harmful input-output pairs are injected into the finetuning data, leading the model to generate unsafe outputs. The potential risks associated with harmful content in finetuning data have been highlighted in several studies [10, 14, 15, 16, 22, 36]. Moreover, parameter-efficient finetuning methods such as LoRA [11] show the safety-degradation even when the finetuning data does not include harmful prompts [21, 33]. The importance of maintaining safety-alignment against these attacks becomes increasingly critical as major AI service providers begin offering Finetuning-as-a-Service. To address this issue, prior works proposed solutions targeting the alignment stage, the finetuning stage, or the post-finetuning stage. First, alignment-stage solutions aim to preemptively enhance robustness against safety-degradation caused by training harmful prompts before performing finetuning. These methods mitigate potential risks through regularization techniques based on expected perturbations [15, 16, 26, 36, 40]. Second, finetuning-stage solutions preserve safety during user-specific downstream task finetuning by freezing safety-critical parameters [22, 23, 45] or incorporating safety-oriented regularization [14, 30, 32]. These approaches often adopt additional alignment data as safety guidance during finetuning. Lastly, post-finetuning-stage solutions focus on analyzing the differences between aligned and finetuned models. Based on their analyses, the model weights are adjusted using various techniques, such as restoring [49], pruning [13] or projection [10], to compensate for the safety-degradation after finetuning. In contrast to prior approaches, we propose a ReFT-based finetuning-stage solution, which filters harmful prompts using the refusal feature and distills alignment knowledge to maintain safety during finetuning.

### 3 Problem Setting

**Scenario.** We assume that Finetuning-as-a-Service providers (i.e., companies that own and deploy LLMs) prioritize model safety. During the alignment stage, service providers are assumed to have access to a dataset containing 5,000 harmful and 5,000 harmless prompts. For each harmful prompt, a corresponding safe response is paired that appropriately refuses the harmful request. Using this dataset, the LLMs are trained to generate a safe refusal response to harmful prompts. During the finetuning stage, users submit custom datasets to the service providers for model customization or jailbreaking. However, the service providers neither have prior knowledge of whether the user data contains harmful prompts, nor access to the distribution of user data during the alignment stage.

**Threat Models.** We assume that user data contains  $p\%$  harmful prompts with harmful responses, while the remaining  $(1 - p)\%$  consists of harmless prompts sampled from the same dataset. When  $p = 0$ , the dataset includes only harmless prompts. Importantly, users do not inform which prompts are harmful or harmless, thereby exposing LLMs to the risk of safety-degradation during finetuning. At the same time, LLMs are expected to maintain strong performance on user-specific downstream tasks while preserving their safety-alignment, making the problem particularly challenging.

### 4 Preliminary: Refusal Feature

The refusal feature, introduced in [3], is a one-dimensional representation associated with refusal responses in safety-aligned LLMs. These features are defined as the mean difference between the feature representations of harmful and harmless prompts at a specific layer. Let  $x^s$  and  $x^{us}$  are safe prompts and unsafe prompts, respectively, and let  $f^l$  denote the features of the last input token

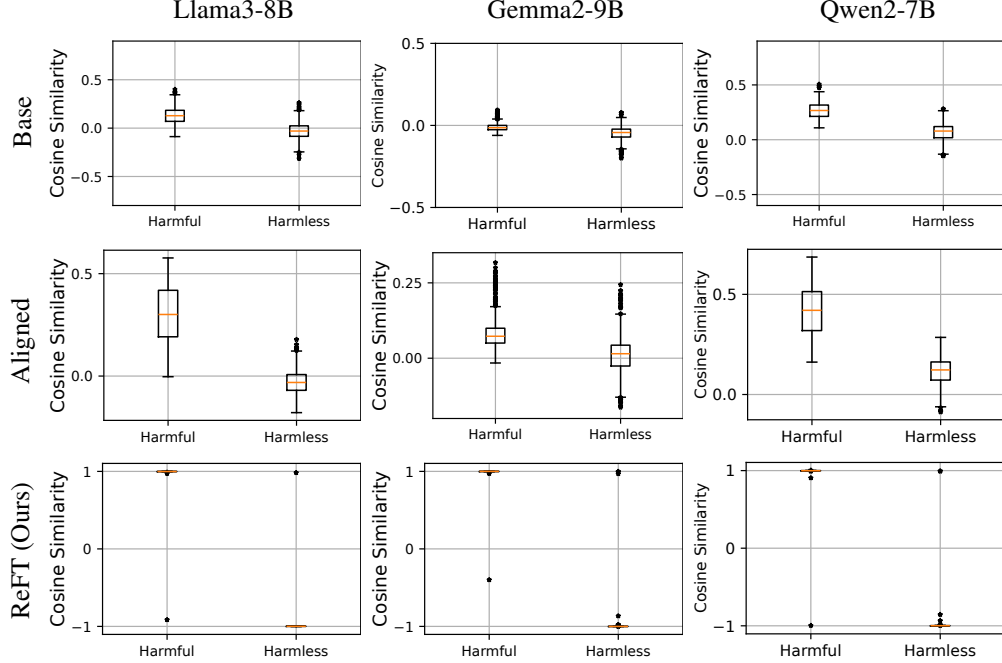


Figure 1: Box plot of cosine similarity distributions for harmful and harmless prompts in the base model, aligned model, and ReFT (Ours). Prompts were sampled from the BeaverTails (harmful,  $n=500$ ) and Alpaca (harmless,  $n=500$ ) datasets, representing diverse general prompts. The sampled prompts visualized here were excluded from the ReFT training set. This visualization highlights that safety-alignment introduces the capability to distinguish harmful from harmless prompts.

Table 1: Accuracy of classifying prompts using refusal features. Prompts with cosine similarity above the threshold are classified as harmful, while those below are classified as harmless.

| Model              | Threshold | Harmful Acc | Harmless Acc | Total Acc |
|--------------------|-----------|-------------|--------------|-----------|
| Llama3-8B          | 0.34      | 86.0%       | 78.8%        | 82.4%     |
| Llama3-8B-Instruct | 0.06      | 95.2%       | 93.6%        | 94.4%     |
| Llama3-8B-ReFT     | 0.97      | 99.8%       | 99.8%        | 99.8%     |
| Gemma2-9B          | -0.037    | 87.8%       | 61.2%        | 74.5%     |
| Gemma2-9B-Instruct | 0.035     | 90.4%       | 70.4%        | 80.4%     |
| Gemma2-9B-ReFT     | 0.97      | 99.8%       | 99.6%        | 99.7%     |
| Qwen2-7B           | 0.15      | 97.6%       | 88.8%        | 93.2%     |
| Qwen2-7B-Instruct  | 0.24      | 93.2%       | 97.2%        | 95.2%     |
| Qwen2-7B-ReFT      | 0.9       | 99.8%       | 99.6%        | 99.7%     |

extracted from a specific layer  $l$  of the LLM. The refusal feature  $R^l$  is computed as follows:

$$R^l = \frac{1}{N_{us}} \sum_{i=1}^{N_{us}} f^l(x_i^{us}) - \frac{1}{N_s} \sum_{i=1}^{N_s} f^l(x_i^s), \quad (1)$$

where  $N_s$  and  $N_{us}$  denote the number of safe and unsafe prompts, respectively. Since safety-aligned LLMs are trained to output refusal responses for harmful prompts and helpful responses for harmless prompts, the mean difference of the features between harmful and harmless prompts extracts only features that are specifically relevant to refusal behaviors. Then, the refusal feature vector  $R^l$  can be interpreted as a refusal direction in the model’s representation space at specific layer  $l$ .

## 5 Observations: Refusal Feature can Classify Harmful/Harmless Prompts

Safety-aligned LLMs are trained on harmful prompts paired with refusal responses and harmless prompts paired with appropriate task-relevant outputs. Then, when harmful prompts that elicit unsafe behavior are provided, the aligned models generate explicit refusal responses (e.g., "I’m sorry, I can’t help with that request."). In contrast, when given harmless prompts, the models produce task-relevant responses. Motivated by these distinct response behaviors, we hypothesize that the internal feature

representations derived from harmful and harmless prompts are distinguishable in safety-aligned LLMs, and this discrimination is reflected in the refusal feature of the aligned models.

To investigate our hypothesis, we measure the similarity between input prompt features and the refusal feature in both base and aligned models, and evaluate whether harmful and harmless prompts can be distinguished based on this similarity. Figure 1 illustrates box plots of cosine similarity distributions for the BeaverTails (harmful) [19] and Alpaca (harmless) data [41]. The results show that aligned models exhibit more distinct similarity distributions, enabling clearer separation between harmful and harmless prompts. In contrast, base models display significant overlap in their similarity distributions, making discrimination between the two types of prompts challenging. Numerically, Table 1 shows that the aligned models achieve higher accuracy than the base model for both harmful and harmless prompts. These findings validate the effectiveness of the refusal feature extracted from safety-aligned models in distinguishing between harmful and harmless prompts.

Motivated by this observation, we develop the Refusal-Feature-guided Teacher (ReFT) model, which is trained to more effectively distinguish between harmful and harmless prompts by leveraging refusal features. As shown in Fig. 1 and Table 1, the ReFT model achieves clearer separation in similarity distributions and higher classification accuracy than both base models and aligned models.

## 6 Method: Refusal-Feature-guided Teacher (ReFT)

Based on our observation that the refusal feature can serve as reliable indicators for classifying harmful and harmless prompts, we train a Refusal-Feature-guided Teacher (ReFT) model and use it for safe finetuning. Unlike prior works, our approach introduces a teacher preparation stage, where the ReFT model is trained, instead of the alignment stage. Subsequently, during finetuning stage, we finetune an unaligned base model directly on user data under the guidance of the ReFT model.

### 6.1 Teacher Preparation Stage

The objective of teacher preparation stage is to train the ReFT model to accurately distinguish between harmful and harmless prompts. To achieve this, we optimize the base model using a safety-alignment loss, which is a supervised finetuning loss computed on a safety-alignment dataset that pairs harmful prompts with refusal responses and harmless prompts with appropriate helpful responses. The alignment loss trains the model to refuse only harmful requests while generate relevant responses to harmless queries, thereby exhibiting distinct behaviors for different prompt types. To further enhance the ReFT model’s discriminative ability, we introduce a regularization term that encourages clearer separation between the features of harmful and harmless prompts, based on their similarity to the refusal feature. Specifically, the regularization term enforces the cosine similarity between the refusal feature and harmful prompt features to approach 1, and the similarity with harmless prompt features to approach  $-1$ . However, overly strong regularization may lead to undesirable internal representations, potentially producing incomprehensible responses. To prevent this, we employ a hyperparameter  $\lambda$  to control the strength of the regularization. The final objective function for teacher preparation stage is defined

---

#### Algorithm 1 Training Process of the ReFT Model

---

**Require:** Unsafe data  $x^{us}$ , Safe data  $x^s$ , Cycle number  $C$ , LoRA weight  $W$ , Regularization strength  $\lambda$ , Learning rate  $\eta$   
**Ensure:** Trained LoRA weight  $W$ , Refusal Feature  $R^l$   
Initialize Unsafe prompt set  $S_{us} \leftarrow []$   
Initialize Safe prompt set  $S_s \leftarrow []$   
Initialize Refusal feature  $R^l \leftarrow None$   
Initialize Counter  $c \leftarrow 0$   
**while** not converged **do**  
    Sample  $B$  examples each of  $x^{us}$  and  $x^s$   
    Append  $x^{us}$  to  $S_{us}$   
    Append  $x^s$  to  $S_s$   
     $c \leftarrow c + B$   
    **if**  $c \geq C$  **then**  
        Compute  $R^l$  from Eq. (1) with  $S_{us}$  and  $S_s$   
        Reset Unsafe prompt set  $S_{us} \leftarrow []$   
        Reset Safe prompt set  $S_s \leftarrow []$   
         $c \leftarrow 0$   
    **end if**  
    **if**  $R^l$  is None **then**  
         $\lambda \leftarrow 0$   
    **end if**  
    Compute  $\mathcal{L}_{teacher}$  from Eq. (2)  
    Update  $W \leftarrow W - \eta \cdot \nabla \mathcal{L}_{teacher}$   
**end while**  
**return**  $W$  and  $R^l$

---

as the combination of the safety-alignment loss and the regularization term:

$$\mathcal{L}_{teacher} = \frac{1}{N} \sum_{i=1}^N \left[ \ell(x_i^s, y_i^s) + \ell(x_i^{us}, y_i^s) + \lambda \{ \|1 + CS(f^l(x_i^s), R^l)\|_2 + \|1 - CS(f^l(x_i^{us}), R^l)\|_2 \} \right], \quad (2)$$

where  $\ell(\cdot, \cdot)$  denotes the cross-entropy loss,  $CS(\cdot, \cdot)$  represents cosine similarity,  $y^s$  is the safe response for each prompt, and  $N$  is the number of training samples. By training the model with Eq. 2, the ReFT model not only effectively distinguishes between harmful and harmless prompts using its refusal feature, but also generates appropriate refusal responses for harmful prompts.

Furthermore, we assume a setting where a pre-aligned model is unavailable, making it impossible to extract refusal features from the aligned models. To address this, we dynamically update the refusal feature during the training of ReFT model at fixed intervals (cycles) using Eq. 1. In each training cycle, harmful and harmless prompts are accumulated into the set  $S_{us}$  and  $S_s$ , respectively. The refusal feature is then recalculated based on these collected prompts. During iterations before the first update cycle, we set  $\lambda = 0$  to disable the regularization, as the refusal feature has not yet been reliably established. This dynamic update of the refusal feature removes the need for a separate alignment stage to obtain the refusal feature, allowing the model to simultaneously compute the refusal feature and learn discriminative features within a single training process, even without access to a pre-aligned model. The complete algorithm for teacher preparation stage is provided in Alg. 1.

## 6.2 Finetuning Stage

In the finetuning stage, the ReFT model is frozen and serves as a teacher for two distinct purposes: (1) filtering harmful prompts in user data and (2) alignment knowledge distillation. This approach enables the base model to effectively learn user-specific tasks while maintaining strong safety-alignment.

First, the ReFT model is employed to filter harmful prompts from user data. Leveraging its capability to distinguish between harmful and harmless prompts, we identify harmful data by measuring the cosine similarity between the refusal feature and the feature of each input prompt. If the similarity exceeds a predefined threshold, the prompt is classified as harmful, otherwise as harmless. This filtering mechanism, based on the ReFT model, is formulated as a binary filtering indicator  $\omega_i$ :

$$\omega_i = \begin{cases} 0, & \text{if } CS(R^l, f^l(x_i)) > \tau \\ 1, & \text{otherwise} \end{cases}, \quad (3)$$

where  $\tau$  is a predefined threshold used to determine harmfulness. In Eq. 3, prompts classified as harmful are excluded from the supervised finetuning loss by setting  $\omega_i = 0$ , since misclassifying harmful prompts as harmless could compromise model safety. Fortunately, as shown in Table 7, the ReFT model misclassifies harmful prompts as harmless less frequently than it misclassifies harmless prompts as harmful. Therefore, we discard all data predicted to be harmful, ensuring that finetuning is performed only on harmless prompts. This strategy effectively preserves model safety by preventing the finetuning of even a small amount of harmful data, which could degrade the safety-alignment.

Secondly, the ReFT model is used to provide soft refusal labels for alignment knowledge distillation. Since our approach directly finetunes an unaligned base model and user data typically lacks harmful prompts with corresponding refusal responses, finetuning solely on user data cannot guarantee model safety. To address this limitation, we reuse the safety-alignment data originally employed during the teacher preparation stage. This strategy eliminates the need to collect additional alignment data specifically for the finetuning stage and ensures that the ReFT model, already trained on this data, can provide accurate refusal responses as soft labels. These soft labels offer more informative supervision and contribute to a smoother loss surface compared to hard labels. As a result, finetuning the base model using soft refusal labels on alignment data enables effective safety-alignment and seamless integration with the supervised finetuning loss on harmless-only user data, allowing the model to reliably learn safe and appropriate responses to harmful inputs.

Overall, our ReFT-based finetuning strategy incorporates the dual-teacher mechanism. The final loss function for the finetuning stage is defined as a combination of the supervised finetuning loss on user

Table 2: Performance under varying harmful prompts ratios  $p$  in user data. Lower harmful scores ( $\downarrow$ ) and higher finetuning accuracy ( $\uparrow$ ) indicate better performance. Results are averaged over seeds 30, 42, and 50. Finetuning accuracy is not reported for  $p = 1.0$  since harmless data is unavailable. Our ReFT-based method consistently achieves the best performance across all harmful ratios.

| Methods       | Harmful Score ( $\downarrow$ ) |                      |                      |                      |                      | Finetune Accuracy ( $\uparrow$ ) |                       |                       |                       |           |
|---------------|--------------------------------|----------------------|----------------------|----------------------|----------------------|----------------------------------|-----------------------|-----------------------|-----------------------|-----------|
|               | clean                          | $p = 0.1$            | $p = 0.3$            | $p = 0.5$            | $p = 1.0$            | clean                            | $p = 0.1$             | $p = 0.3$             | $p = 0.5$             | $p = 1.0$ |
| SFT           | 2.2 $\pm$ 0.1                  | 16.2 $\pm$ 0.4       | 57.3 $\pm$ 0.6       | 71.3 $\pm$ 0.6       | 76.7 $\pm$ 0.4       | 41.1 $\pm$ 0.0                   | 39.9 $\pm$ 0.6        | 39.1 $\pm$ 0.2        | 37.1 $\pm$ 0.6        | -         |
| Repnoise [36] | 2.7 $\pm$ 0.4                  | 29.9 $\pm$ 0.6       | 67.0 $\pm$ 5.1       | 75.7 $\pm$ 3.1       | 79.7 $\pm$ 0.6       | 37.4 $\pm$ 0.3                   | 37.0 $\pm$ 1.2        | 36.3 $\pm$ 0.7        | 36.0 $\pm$ 1.4        | -         |
| Vaccine [16]  | 1.3 $\pm$ 0.2                  | 5.4 $\pm$ 0.7        | 35.0 $\pm$ 0.3       | 57.5 $\pm$ 0.4       | 81.3 $\pm$ 0.1       | 22.9 $\pm$ 0.5                   | 23.2 $\pm$ 1.0        | 21.7 $\pm$ 0.3        | 20.3 $\pm$ 0.4        | -         |
| Booster [15]  | 2.3 $\pm$ 0.1                  | 5.9 $\pm$ 0.2        | 65.1 $\pm$ 0.3       | 75.0 $\pm$ 0.6       | 79.0 $\pm$ 0.4       | 44.5 $\pm$ 0.5                   | 44.0 $\pm$ 0.9        | 44.4 $\pm$ 0.6        | 43.5 $\pm$ 0.6        | -         |
| LDIFS [30]    | 1.0 $\pm$ 0.2                  | 4.1 $\pm$ 0.7        | 7.1 $\pm$ 0.2        | 14.7 $\pm$ 0.3       | 24.0 $\pm$ 0.4       | 18.0 $\pm$ 0.9                   | 16.7 $\pm$ 0.8        | 15.5 $\pm$ 0.1        | 15.4 $\pm$ 0.6        | -         |
| Lisa [14]     | 1.4 $\pm$ 0.2                  | 5.3 $\pm$ 0.1        | 25.9 $\pm$ 1.5       | 49.2 $\pm$ 0.7       | 67.3 $\pm$ 1.0       | 38.3 $\pm$ 0.7                   | 38.9 $\pm$ 0.9        | 37.8 $\pm$ 0.9        | 36.2 $\pm$ 0.5        | -         |
| ReFT (Ours)   | <b>0.9</b> $\pm$ 0.3           | <b>1.0</b> $\pm$ 0.5 | <b>0.6</b> $\pm$ 0.1 | <b>0.9</b> $\pm$ 0.3 | <b>1.3</b> $\pm$ 0.2 | <b>48.8</b> $\pm$ 0.5            | <b>49.0</b> $\pm$ 0.5 | <b>45.5</b> $\pm$ 0.9 | <b>44.8</b> $\pm$ 0.5 | -         |

data and the alignment distillation loss on safety-alignment data:

$$\mathcal{L}_{ft} = \frac{1}{N_{user}} \sum_{i=1}^{N_{user}} \omega_i * \ell(x_i, y_i) + \alpha T^2 * \frac{1}{N_{align}} \sum_{i=1}^{N_{align}} \text{KL}(p_{t,i}^T || p_{s,i}^T). \quad (4)$$

In the supervised finetuning loss,  $\ell(x_i, y_i)$  denotes the cross-entropy loss on user data  $(x_i, y_i)$ . In the alignment distillation loss, KL denotes KL-divergence computed on alignment data, and  $p_{t,i}^T$  and  $p_{s,i}^T$  represent the softmax logits of the teacher (ReFT) and student (base) models, respectively, with temperature  $T$ . These are defined as  $p_i^T = \frac{\exp(z_i/T)}{\sum_{j=1}^V \exp(z_j/T)}$  where  $z$  denotes the model logits and  $V$  is the vocabulary size. Additionally, the hyperparameter  $\alpha$  controls the weight of the distillation.

## 7 Experiment

We evaluate the effectiveness of our ReFT-based finetuning strategy in terms of safety-alignment and user-specific task performance under various experimental settings. We varied the ratio of harmful prompts, the size of user data, the type of harmless prompts (GSM8K [7], SST2 [39], AGNEWS [51], AlpacaEval [25]), and the base model (Llama3-8B [2], Gemma2-9B [42], Qwen2-7B [1]). Unless noted otherwise, we used Llama3-8B, 0.1 poison ratio, 1000 user data, and GSM8K as harmless data.

**Datasets.** During the teacher preparation stage, we used  $N = 5,000$  harmful prompts with corresponding refusal responses from the BeaverTails dataset [19], and  $N = 5,000$  harmless data with helpful responses from the Alpaca dataset [41]. For the finetuning stage, the user data was constructed by mixing harmful and harmless data with a specific poison ratio. The number of alignment data used during finetuning stage, denoted  $N_{align}$ , was set equal to the number of user data  $N_{user}$ . Although all harmful prompts used in our experiments were sourced from the BeaverTails dataset, we used distinct subsets for the teacher preparation, finetuning, and evaluation stages to prevent any data overlapping.

**Metrics.** To evaluate both safety-alignment and user-specific task performance, we adopt two metrics: Harmful Score (HS) and Finetuning Accuracy (FA), following prior works [16, 15, 14]. HS is defined as the proportion of harmful responses among 1,000 outputs generated from the BeaverTails test set, classifying harmfulness by the pretrained moderation model Beaver-Dam-7B [19]. In contrast, FA is measured by a task-specific finetuning accuracy on downstream benchmarks including GSM8K, SST2, AGNEWS, and AlpacaEval, using 872, 1,000, 1,000, and 122 samples from their respective test sets. For AlpacaEval, the accuracy was assessed by GPT-4o model [18], following standard evaluation practices [25]. Notably, both HS and FA were evaluated after the finetuning stage.

### 7.1 Experiment Results

**Robustness under Varying Harmful Prompt Ratio.** We evaluate the effectiveness of our ReFT-based finetuning strategy by measuring both harmful score and finetuning accuracy under varying ratios of harmful prompts  $p$  in user data, ranging from fully clean data ( $p = 0$ ) to entirely harmful data ( $p = 1.0$ ). Table 2 shows that our method consistently achieves the lowest harmful score and the highest finetuning accuracy across all values of  $p$ , outperforming all baselines. This superior performance stems from our effective harmful data filtering using the ReFT model, which allows the

Table 3: Performance comparison across varying amounts of user data. Our method consistently outperforms the baselines in both harmful score and finetuning accuracy, highlighting its scalability.

| Methods       | Harmful Score ( $\downarrow$ ) |            |            |            |            | Finetune Accuracy ( $\uparrow$ ) |             |             |             |             |
|---------------|--------------------------------|------------|------------|------------|------------|----------------------------------|-------------|-------------|-------------|-------------|
|               | n=1000                         | n=1500     | n=2000     | n=2500     | Average    | n=1000                           | n=1500      | n=2000      | n=2500      | Average     |
| SFT           | 16.7                           | 39.4       | 55.8       | 63.9       | 44.0       | 40.6                             | 42.9        | 44.5        | 45.3        | 43.3        |
| Repnoise [36] | 30.4                           | 50.4       | 61.7       | 72.9       | 53.9       | 38.4                             | 40.5        | 43.6        | 43.5        | 41.5        |
| Vaccine [16]  | 4.8                            | 19.8       | 34.1       | 45.0       | 25.9       | 24.4                             | 28.5        | 31.3        | 33.9        | 29.5        |
| Booster [15]  | 5.9                            | 19.4       | 48.2       | 62.6       | 34.0       | 43.4                             | 45.3        | 48.4        | 48.5        | 46.4        |
| LDIFS [30]    | 4.0                            | 5.7        | 4.7        | 6.0        | 5.1        | 17.0                             | 16.7        | 17.7        | 18.4        | 17.5        |
| Lisa [14]     | 5.3                            | 8.2        | 10.4       | 12.8       | 9.2        | 38.3                             | 37.8        | 40.3        | 42.7        | 39.8        |
| ReFT (Ours)   | <b>0.5</b>                     | <b>0.9</b> | <b>0.9</b> | <b>1.0</b> | <b>0.8</b> | <b>49.0</b>                      | <b>50.1</b> | <b>52.1</b> | <b>51.8</b> | <b>50.8</b> |

Table 4: Performance comparison across different downstream datasets for finetuning. The results demonstrates strong safety-alignment and generalization performance of our finetuning strategy.

| Methods       | GSM8K           |               | SST2            |               | AGNEWS          |               | AlpacaEval      |               | Average         |               |
|---------------|-----------------|---------------|-----------------|---------------|-----------------|---------------|-----------------|---------------|-----------------|---------------|
|               | HS $\downarrow$ | FA $\uparrow$ | HS $\downarrow$ | FA $\uparrow$ | HS $\downarrow$ | FA $\uparrow$ | HS $\downarrow$ | FA $\uparrow$ | HS $\downarrow$ | FA $\uparrow$ |
| SFT           | 16.7            | 40.6          | 33.5            | 93.4          | 28.2            | 82.8          | 23.7            | 32.7          | 20.4            | 49.9          |
| Repnoise [36] | 30.4            | 38.4          | 63.0            | 93.4          | 58.6            | 84.6          | 45.4            | 29.3          | 39.5            | 49.1          |
| Vaccine [16]  | 4.8             | 24.4          | 35.8            | 90.0          | 29.5            | 83.2          | 55.8            | 14.4          | 25.2            | 42.4          |
| Booster [15]  | 5.9             | 43.4          | 9.2             | 93.6          | 5.3             | 85.3          | 29.4            | 34.0          | 10.0            | 51.3          |
| LDIFS [30]    | 4.0             | 17.0          | 14.6            | 90.5          | 12.5            | 71.2          | 5.7             | 33.7          | 7.4             | 42.5          |
| Lisa [14]     | 5.3             | 38.3          | 21.4            | 93.4          | 14.9            | 84.5          | 10.1            | 29.6          | 10.3            | 49.2          |
| ReFT (Ours)   | <b>0.5</b>      | <b>49.0</b>   | <b>1.3</b>      | <b>94.5</b>   | <b>1.2</b>      | <b>86.1</b>   | <b>2.4</b>      | <b>34.6</b>   | <b>1.1</b>      | <b>52.8</b>   |

base model to finetune only on helpful user data, even when the user data contains a large number of harmful prompts. In addition, we observe that alignment-stage baselines such as RepNoise [36], Vaccine [16], and Booster [15] are vulnerable to high harmful ratios ( $p \geq 0.3$ ), which corresponds to scenarios where malicious users attempt to jailbreak LLMs via harmful finetuning attacks. In contrast, finetuning-stage solutions such as LDIFS [30], Lisa [14], and our approach remain robustness even under high harmful ratios, consistently achieving lower harmful scores. Among these, our method yields the best performance in both safety-alignment and user-specific downstream tasks.

**Scalability under Varying the Number of User Data.** To evaluate how performance varies with an increasing amount of user data, we measured both harmful score and finetuning accuracy as the number of user data samples increases from 500 to 2,000. As shown in Table 3, our finetuning strategy based on the ReFT model consistently achieves the best performance across all cases, aligned with the results in Table 2. Specifically, given a fixed poison ratio, our method maintains a low harmful score even as the absolute number of harmful prompts increases proportionally with the size of the user data, demonstrating strong robustness in safety-alignment. Simultaneously, finetuning accuracy improves as more user data for user-specific tasks becomes available. These experimental results validate the scalability and adaptability of our approach across varying data scales.

**Generalization across Diverse Finetuning Datasets.** In our default setting, we used GSM8K dataset as user-specific downstream task. To further evaluate the generalization ability of our finetuning strategy across diverse downstream tasks, we replaced the harmless portion of user data with samples from SST2, AGNEWS, and AlpacaEval datasets. We then measured both harmful score and finetuning accuracy for our method and baseline approaches. Table 4 presents that our approach achieves the lowest harmful score and the highest finetuning accuracy across all datasets. These results demonstrate the effectiveness of our ReFT-based data filtering, even when the harmless data is sampled from different distributions. Overall, our method exhibits strong generalization across a wide range of user-specific tasks, making it practically applicable in real-world scenarios.

**Adaptability across Model Architectures.** We evaluate the adaptability of our finetuning strategy to diverse model architectures by training the ReFT model on both Gemma2-9B and Qwen2-7B architectures, and subsequently finetuning each corresponding base model using the trained ReFT model. Table 5 shows that our approach reliably reduces harmfulness and improves user-specific downstream task performance across architectures. This strong performance is attributed to the high classification accuracy of our ReFT-based harmful prompt filtering mechanism across model architectures, as illustrated in Fig. 1 and Table 1. These results indicate that our method is not only effective for a specific model architecture but also generalizes well across various LLM backbones.



Table 5: Performance comparison across different model architectures. Our ReFT-based finetuning strategy shows strong adaptability across Llama3-8B, Gemma2-9B, and Qwen2-7B.

| Methods       | Llama3-8B  |             | Gemma2-9B  |             | Qwen2-7B   |             | Average    |             |
|---------------|------------|-------------|------------|-------------|------------|-------------|------------|-------------|
|               | HS ↓       | FA ↑        | HS ↓       | FA ↑        | HS ↓       | FA ↑        | HS ↓       | FA ↑        |
| SFT           | 16.7       | 40.6        | 26.4       | 59.5        | 37.9       | 66.8        | 27.0       | 55.6        |
| Repnoise [36] | 30.4       | 38.4        | 26.2       | 57.1        | 25.4       | 63.7        | 27.3       | 53.1        |
| Vaccine [16]  | 4.8        | 24.4        | 18.0       | 52.5        | 10.2       | 63.6        | 11.0       | 46.8        |
| Booster [15]  | 5.9        | 43.4        | 2.3        | 58.4        | 4.9        | <b>70.0</b> | 4.4        | 57.3        |
| LDIFS [30]    | 4.0        | 17.0        | 3.1        | 36.0        | 10.7       | 64.1        | 5.9        | 39.0        |
| Lisa [14]     | 5.3        | 38.3        | 6.2        | 54.5        | 4.4        | 61.6        | 5.3        | 51.5        |
| ReFT (Ours)   | <b>0.5</b> | <b>49.0</b> | <b>1.3</b> | <b>63.6</b> | <b>0.6</b> | 69.7        | <b>0.8</b> | <b>60.8</b> |

Table 6: Effects of applying ReFT-based finetuning to alignment-stage solutions.

| Methods       | HS ↓       | FA ↑        |
|---------------|------------|-------------|
| SFT           | 16.7       | 40.6        |
| SFT+ReFT      | <b>1.1</b> | <b>42.1</b> |
| Repnoise [36] | 30.4       | 38.4        |
| Repnoise+ReFT | <b>1.4</b> | <b>39.2</b> |
| Vaccine [16]  | 4.8        | <b>24.4</b> |
| Vaccine+ReFT  | <b>2.2</b> | 22.0        |
| Booster [15]  | 5.9        | 43.4        |
| Booster+ReFT  | <b>1.9</b> | <b>43.8</b> |

## 7.2 Analysis

**Reinforcing Alignment-stage Solutions with ReFT-based Finetuning Strategy.** To identify whether our ReFT-based finetuning strategy can further enhance the safety and user-specific task performance of aligned models from alignment-stage techniques, we apply our method to these aligned models during finetuning stage and measure both the harmful score and finetuning accuracy. As shown in Table 6, our approach significantly reduces the harmful score while maintaining comparable finetuning accuracy in most cases. The reinforced safety-alignment demonstrates that ReFT-based data filtering and alignment distillation can complement the alignment-stage solutions.

**Classification Accuracy during Finetuning.** Beyond the results presented in Fig. 1 and Table 1, we evaluate the classification accuracy between harmful and harmless data during finetuning across GSM8K, SST2, AGNEWS, and AlpacaEval. Table 7 reports that our ReFT-based classification identifies harmful prompts with near-perfect accuracy and achieves high accuracy for harmless prompts across diverse datasets. The strong classification accuracy supports the reliable harmful data filtering in user data, regardless of the data distribution, preventing harmful prompts from being used in finetuning.

Table 7: Classification accuracy for harmful and harmless prompts in user data during finetuning.

| Datasets   | Harmful | Harmless | Total  |
|------------|---------|----------|--------|
| GSM8K      | 100.00% | 97.70%   | 97.93% |
| SST2       | 99.91%  | 95.30%   | 95.76% |
| AGNEWS     | 99.91%  | 99.86%   | 99.87% |
| AlpacaEval | 99.90%  | 77.04%   | 79.33% |

### Effect of Each Component in ReFT-based Finetuning Strategy.

Our ReFT-based finetuning method consists of two components: harmful data filtering (Filtering) and alignment distillation (AD) using the ReFT model. To evaluate their individual and combined contributions, we conduct an ablation study by selectively removing each component. When Filtering is omitted, the model is finetuned on both harmful and harmless prompts in user data. When AD is excluded, the model is trained using hard-labeled alignment data. As shown in Table 8, Filtering improves both harmful score and finetuning accuracy by preventing the model from being finetuned on harmful prompts. In contrast, AD further enhances these metrics by providing soft refusal labels, which smooth the alignment loss surface and offer richer supervision for harmful prompt. Consequently, combining Filtering and AD allows our method to achieve high user-specific task performance while preserving safety-alignment.

Table 8: Ablation study evaluating the individual contributions of Filtering and AD.

| Filtering | AD | HS ↓ | FA ↑ |
|-----------|----|------|------|
| X         | X  | 14.0 | 48.7 |
| O         | X  | 0.7  | 47.3 |
| X         | O  | 8.9  | 46.6 |
| O         | O  | 0.5  | 49.0 |

**Hyperparameters.** Experiments to identify the optimal hyperparameters for our ReFT-based finetuning method, including the cycle number  $C$ , regularization strength  $\lambda$ , threshold value  $\tau$ , distillation temperature  $T$ , distillation weight  $\alpha$  and the layer index  $l$ , are reported in Supplementary Materials.

**Limitation.** Our finetuning strategy relies on the ReFT model’s ability to accurately classify harmful and harmless prompts based on its refusal feature. Therefore, safety-alignment may be compromised if adversarial attacks are developed that target the ReFT model to disrupt its refusal feature.

## 8 Conclusion

In this work, we address the safety risks of Finetuning-as-a-Service, where the safety-alignment of LLMs can be compromised by finetuning on even a few harmful prompts in user data. Motivated by

our observation that the refusal feature of safety-aligned models can distinguish between harmful and harmless prompts, we introduce the Refusal-Feature-based Teacher (ReFT) model, which accurately identifies harmful prompts and generates appropriate refusal responses. During finetuning, the ReFT model serves as a teacher, performing data filtering and alignment distillation. Our extensive experiments demonstrate that our ReFT-based finetuning strategy consistently achieves the lowest harmful score and the highest finetuning accuracy across various settings, outperforming existing baselines. In conclusion, our approach offers a promising solution for safe and effective Finetuning-as-a-Service, ensuring high user-specific task performance while preserving safety-alignment.

## References

- [1] Qwen2 technical report. 2024.
- [2] AI@Meta. Llama 3 model card. 2024.
- [3] Andy Arditi, Oscar Obeso, Aaquib Syed, Daniel Paleka, Nina Panickssery, Wes Gurnee, and Neel Nanda. Refusal in language models is mediated by a single direction. *arXiv preprint arXiv:2406.11717*, 2024.
- [4] Somnath Banerjee, Sayan Layek, Soham Tripathy, Shanu Kumar, Animesh Mukherjee, and Rima Hazra. Safeinfer: Context adaptive decoding time safety alignment for large language models. In *Proceedings of the AAAI Conference on Artificial Intelligence*, volume 39, pages 27188–27196, 2025.
- [5] Federico Bianchi, Mirac Suzgun, Giuseppe Attanasio, Paul Röttger, Dan Jurafsky, Tatsunori Hashimoto, and James Zou. Safety-tuned llamas: Lessons from improving the safety of large language models that follow instructions. *arXiv preprint arXiv:2309.07875*, 2023.
- [6] Patrick Chao, Alexander Robey, Edgar Dobriban, Hamed Hassani, George J Pappas, and Eric Wong. Jailbreaking black box large language models in twenty queries. *arXiv preprint arXiv:2310.08419*, 2023.
- [7] Karl Cobbe, Vineet Kosaraju, Mohammad Bavarian, Mark Chen, Heewoo Jun, Lukasz Kaiser, Matthias Plappert, Jerry Tworek, Jacob Hilton, Reiichiro Nakano, Christopher Hesse, and John Schulman. Training verifiers to solve math word problems. *arXiv preprint arXiv:2110.14168*, 2021.
- [8] Yanrui Du, Sendong Zhao, Danyang Zhao, Ming Ma, Yuhang Chen, Liangyu Huo, Qing Yang, Dongliang Xu, and Bing Qin. Mogu: A framework for enhancing safety of open-sourced llms while preserving their usability. *arXiv preprint arXiv:2405.14488*, 2024.
- [9] Daya Guo, Dejian Yang, Haowei Zhang, Junxiao Song, Ruoyu Zhang, Runxin Xu, Qihao Zhu, Shitong Ma, Peiyi Wang, Xiao Bi, et al. Deepseek-r1: Incentivizing reasoning capability in llms via reinforcement learning. *arXiv preprint arXiv:2501.12948*, 2025.
- [10] Chia-Yi Hsu, Yu-Lin Tsai, Chih-Hsun Lin, Pin-Yu Chen, Chia-Mu Yu, and Chun-Ying Huang. Safe lora: The silver lining of reducing safety risks when finetuning large language models. *Advances in Neural Information Processing Systems*, 37:65072–65094, 2024.
- [11] Edward J Hu, Yelong Shen, Phillip Wallis, Zeyuan Allen-Zhu, Yuanzhi Li, Shean Wang, Lu Wang, Weizhu Chen, et al. Lora: Low-rank adaptation of large language models. *ICLR*, 1(2):3, 2022.
- [12] Xiaomeng Hu, Pin-Yu Chen, and Tsung-Yi Ho. Gradient cuff: Detecting jailbreak attacks on large language models by exploring refusal loss landscapes. *arXiv preprint arXiv:2403.00867*, 2024.
- [13] Tiansheng Huang, Gautam Bhattacharya, Pratik Joshi, Josh Kimball, and Ling Liu. Antidote: Post-fine-tuning safety alignment for large language models against harmful fine-tuning. *arXiv preprint arXiv:2408.09600*, 2024.
- [14] Tiansheng Huang, Sihao Hu, Fatih Ilhan, Selim Tekin, and Ling Liu. Lisa: Lazy safety alignment for large language models against harmful fine-tuning attack. *Advances in Neural Information Processing Systems*, 37:104521–104555, 2024.

- [15] Tiansheng Huang, Sihao Hu, Fatih Ilhan, Selim Furkan Tekin, and Ling Liu. Booster: Tackling harmful fine-tuning for large language models via attenuating harmful perturbation. *arXiv preprint arXiv:2409.01586*, 2024.
- [16] Tiansheng Huang, Sihao Hu, and Ling Liu. Vaccine: Perturbation-aware alignment for large language models against harmful fine-tuning attack. *arXiv preprint arXiv:2402.01109*, 2024.
- [17] Kuo-Han Hung, Ching-Yun Ko, Ambrish Rawat, I Chung, Winston H Hsu, Pin-Yu Chen, et al. Attention tracker: Detecting prompt injection attacks in llms. *arXiv preprint arXiv:2411.00348*, 2024.
- [18] Aaron Hurst, Adam Lerer, Adam P Goucher, Adam Perelman, Aditya Ramesh, Aidan Clark, AJ Ostrow, Akila Welihinda, Alan Hayes, Alec Radford, et al. Gpt-4o system card. *arXiv preprint arXiv:2410.21276*, 2024.
- [19] Jiaming Ji, Mickel Liu, Josef Dai, Xuehai Pan, Chi Zhang, Ce Bian, Boyuan Chen, Ruiyang Sun, Yizhou Wang, and Yaodong Yang. Beavertails: Towards improved safety alignment of llm via a human-preference dataset. *Advances in Neural Information Processing Systems*, 36:24678–24704, 2023.
- [20] Albert Qiaochu Jiang, Alexandre Sablayrolles, Arthur Mensch, Chris Bamford, Devendra Singh Chaplot, Diego de Las Casas, Florian Bressand, Gianna Lengyel, Guillaume Lample, Lucile Saulnier, L’elio Renard Lavaud, Marie-Anne Lachaux, Pierre Stock, Teven Le Scao, Thibaut Lavril, Thomas Wang, Timothée Lacroix, and William El Sayed. Mistral 7b. *ArXiv*, abs/2310.06825, 2023.
- [21] Simon Lermen, Charlie Rogers-Smith, and Jeffrey Ladish. Lora fine-tuning efficiently undoes safety training in llama 2-chat 70b. *arXiv preprint arXiv:2310.20624*, 2023.
- [22] Mingjie Li, Wai Man Si, Michael Backes, Yang Zhang, and Yisen Wang. Salora: Safety-alignment preserved low-rank adaptation. *arXiv preprint arXiv:2501.01765*, 2025.
- [23] Shen Li, Liuyi Yao, Lan Zhang, and Yaliang Li. Safety layers in aligned large language models: The key to llm security. *arXiv preprint arXiv:2408.17003*, 2024.
- [24] Xiao Li, Zhuhong Li, Qiongxiu Li, Bingze Lee, Jinghao Cui, and Xiaolin Hu. Faster-gcg: Efficient discrete optimization jailbreak attacks against aligned large language models. *arXiv preprint arXiv:2410.15362*, 2024.
- [25] Xuechen Li, Tianyi Zhang, Yann Dubois, Rohan Taori, Ishaan Gulrajani, Carlos Guestrin, Percy Liang, and Tatsunori B. Hashimoto. AlpacaEval: An automatic evaluator of instruction-following models. [https://github.com/tatsu-lab/alpaca\\_eval](https://github.com/tatsu-lab/alpaca_eval), 5 2023.
- [26] Guozhi Liu, Weiwei Lin, Tiansheng Huang, Ruichao Mo, Qi Mu, and Li Shen. Targeted vaccine: Safety alignment for large language models against harmful fine-tuning via layer-wise perturbation. *arXiv preprint arXiv:2410.09760*, 2024.
- [27] Xiaogeng Liu, Nan Xu, Muhao Chen, and Chaowei Xiao. Autodan: Generating stealthy jailbreak prompts on aligned large language models. *arXiv preprint arXiv:2310.04451*, 2023.
- [28] AI @ Meta Llama Team. The llama 3 herd of models, 2024.
- [29] Ilya Loshchilov and Frank Hutter. Decoupled weight decay regularization. *arXiv preprint arXiv:1711.05101*, 2017.
- [30] Jishnu Mukhoti, Yarin Gal, Philip HS Torr, and Puneet K Dokania. Fine-tuning can cripple your foundation model; preserving features may be the solution. *arXiv preprint arXiv:2308.13320*, 2023.
- [31] Long Ouyang, Jeffrey Wu, Xu Jiang, Diogo Almeida, Carroll Wainwright, Pamela Mishkin, Chong Zhang, Sandhini Agarwal, Katarina Slama, Alex Ray, et al. Training language models to follow instructions with human feedback. *Advances in neural information processing systems*, 35:27730–27744, 2022.

- [32] et al. Qi. Constrain-sft: A supervised fine-tuning approach to enhance safety alignment in large language models. *Proceedings of NeurIPS 2024*, 37:95174, 2024.
- [33] Xiangyu Qi, Yi Zeng, Tinghao Xie, Pin-Yu Chen, Ruoxi Jia, Prateek Mittal, and Peter Henderson. Fine-tuning aligned language models compromises safety, even when users do not intend to! *arXiv preprint arXiv:2310.03693*, 2023.
- [34] Rafael Rafailov, Archit Sharma, Eric Mitchell, Christopher D Manning, Stefano Ermon, and Chelsea Finn. Direct preference optimization: Your language model is secretly a reward model. *Advances in Neural Information Processing Systems*, 36:53728–53741, 2023.
- [35] LG Research, Kyunghoon Bae, Eunbi Choi, Kibong Choi, Stanley Jungkyu Choi, Yemuk Choi, Seokhee Hong, Junwon Hwang, Hyojin Jeon, Kijeong Jeon, et al. Exaone deep: Reasoning enhanced language models. *arXiv preprint arXiv:2503.12524*, 2025.
- [36] Domenic Rosati, Jan Wehner, Kai Williams, Lukasz Bartoszcze, Robie Gonzales, Subhabrata Majumdar, Hassan Sajjad, Frank Rudzicz, et al. Representation noising: A defence mechanism against harmful finetuning. *Advances in Neural Information Processing Systems*, 37:12636–12676, 2024.
- [37] Abhay Sheshadri, Aidan Ewart, Phillip Guo, Aengus Lynch, Cindy Wu, Vivek Hebbar, Henry Sleight, Asa Cooper Stickland, Ethan Perez, Dylan Hadfield-Menell, et al. Targeted latent adversarial training improves robustness to persistent harmful behaviors in llms. *arXiv e-prints*, pages arXiv–2407, 2024.
- [38] Abhay Sheshadri, Aidan Ewart, Phillip Guo, Aengus Lynch, Cindy Wu, Vivek Hebbar, Henry Sleight, Asa Cooper Stickland, Ethan Perez, Dylan Hadfield-Menell, et al. Latent adversarial training improves robustness to persistent harmful behaviors in llms. *arXiv preprint arXiv:2407.15549*, 2024.
- [39] Richard Socher, Alex Perelygin, Jean Wu, Jason Chuang, Christopher D. Manning, Andrew Ng, and Christopher Potts. Recursive deep models for semantic compositionality over a sentiment treebank. In *Proceedings of the 2013 Conference on Empirical Methods in Natural Language Processing*, pages 1631–1642, Seattle, Washington, USA, October 2013. Association for Computational Linguistics.
- [40] Rishub Tamirisa, Bhruhu Bharathi, Long Phan, Andy Zhou, Alice Gatti, Tarun Suresh, Maxwell Lin, Justin Wang, Rowan Wang, Ron Arel, et al. Tamper-resistant safeguards for open-weight llms. *arXiv preprint arXiv:2408.00761*, 2024.
- [41] Rohan Taori, Ishaan Gulrajani, Tianyi Zhang, Yann Dubois, Xuechen Li, Carlos Guestrin, Percy Liang, and Tatsunori B. Hashimoto. Stanford alpaca: An instruction-following llama model. [https://github.com/tatsu-lab/stanford\\_alpaca](https://github.com/tatsu-lab/stanford_alpaca), 2023.
- [42] Gemma Team, Morgane Riviere, Shreya Pathak, Pier Giuseppe Sessa, Cassidy Hardin, Surya Bhupatiraju, Léonard Hussenot, Thomas Mesnard, Bobak Shahriari, Alexandre Ramé, et al. Gemma 2: Improving open language models at a practical size. *arXiv preprint arXiv:2408.00118*, 2024.
- [43] Hugo Touvron, Thibaut Lavril, Gautier Izacard, Xavier Martinet, Marie-Anne Lachaux, Timothée Lacroix, Baptiste Rozière, Naman Goyal, Eric Hambro, Faisal Azhar, et al. Llama: Open and efficient foundation language models. *arXiv preprint arXiv:2302.13971*, 2023.
- [44] Xunguang Wang, Daoyuan Wu, Zhenlan Ji, Zongjie Li, Pingchuan Ma, Shuai Wang, Yingjiu Li, Yang Liu, Ning Liu, and Juergen Rahmel. Selfdefend: Llms can defend themselves against jailbreaking in a practical manner. *arXiv preprint arXiv:2406.05498*, 2024.
- [45] et al. Wei. Freeze: A method to preserve safety alignment during fine-tuning of large language models. *Proceedings of NeurIPS 2024*, 37:96357, 2024.
- [46] Sophie Xhonneux, Alessandro Sordoni, Stephan Günemann, Gauthier Gidel, and Leo Schwinn. Efficient adversarial training in llms with continuous attacks. *arXiv preprint arXiv:2405.15589*, 2024.

- [47] Yueqi Xie, Minghong Fang, Renjie Pi, and Neil Gong. Gradsafe: Detecting jailbreak prompts for llms via safety-critical gradient analysis. *arXiv preprint arXiv:2402.13494*, 2024.
- [48] Zhangchen Xu, Fengqing Jiang, Luyao Niu, Jinyuan Jia, Bill Yuchen Lin, and Radha Pooven-dran. Safedecoding: Defending against jailbreak attacks via safety-aware decoding. *arXiv preprint arXiv:2402.08983*, 2024.
- [49] Xin Yi, Shunfan Zheng, Linlin Wang, Gerard de Melo, Xiaoling Wang, and Liang He. Nlsr: Neuron-level safety realignment of large language models against harmful fine-tuning. In *Proceedings of the AAAI Conference on Artificial Intelligence*, volume 39, pages 25706–25714, 2025.
- [50] Lei Yu, Virginie Do, Karen Hambardzumyan, and Nicola Cancedda. Robust llm safeguarding via refusal feature adversarial training. *arXiv preprint arXiv:2409.20089*, 2024.
- [51] Xiang Zhang, Junbo Jake Zhao, and Yann LeCun. Character-level convolutional networks for text classification. In *NIPS*, 2015.
- [52] Yuqi Zhang, Liang Ding, Lefei Zhang, and Dacheng Tao. Intention analysis makes llms a good jailbreak defender. *arXiv preprint arXiv:2401.06561*, 2024.
- [53] Zhengyue Zhao, Xiaoyun Zhang, Kaidi Xu, Xing Hu, Rui Zhang, Zidong Du, Qi Guo, and Yunji Chen. Adversarial contrastive decoding: Boosting safety alignment of large language models via opposite prompt optimization. *arXiv preprint arXiv:2406.16743*, 2024.
- [54] Andy Zou, Long Phan, Justin Wang, Derek Duenas, Maxwell Lin, Maksym Andriushchenko, J Zico Kolter, Matt Fredrikson, and Dan Hendrycks. Improving alignment and robustness with circuit breakers. In *The Thirty-eighth Annual Conference on Neural Information Processing Systems*, 2024.
- [55] Andy Zou, Zifan Wang, J. Zico Kolter, and Matt Fredrikson. Universal and transferable adversarial attacks on aligned language models, 2023.

# Supplementary Material

## A Experiment Details

### A.1 Training Setup

In the teacher preparation stage, we train the Refusal-Feature-guided Teacher (ReFT) model for 20 epochs using batches of size 10, consisting of 5 harmful and 5 harmless prompts, with a learning rate of  $5e^{-4}$ . During the finetuning stage, we train the base model with ReFT for 20 epochs using 20 batches (10 harmful data and 10 harmless data), with a learning rate of  $1e^{-5}$ . For the AlpacaEval dataset [25], due to its small size, we train the base model for 100 epochs using 700 prompts. In both stages, we apply LoRA [11] with a rank of 32, targeting the query, key, and value components of the attention modules. Also, we use the AdamW optimizer [29] with a weight decay of 0.1 and a constant learning rate schedule.

### A.2 Hyperparameters for Our Method

Our proposed method introduces several additional hyperparameters. First, in teacher preparation stage, we set the regularization strength for training ReFT model to  $\lambda = 0.1$ . Refusal features are extracted from specific layer in LLMs:  $l = 12$  for LLAMA3-8B,  $l = 11$  for Gemma2-9B,  $l = 18$  for Qwen2-7B. The refusal features are updated periodically every  $C = 6$  cycles, with each update performed using 30 harmful and 30 harmless prompts. During finetuning stage, for harmful and harmless classification using the ReFT model, we use a threshold of 0.9 to maximize the recall of harmful prompts. For alignment knowledge distillation, we set the distillation strength  $\alpha = 0.1$  and use a the temperature  $T = 1$ . Ablation studies to identify the optimal values for these hyperparameters are presented in Sec. B. All the other hyperparameters for the baseline methods follow the settings specified in their respective original papers [15, 16, 30, 14, 36].

## B Experiments for Finding Optimal Hyperparameters

### B.1 Layer Selection for Refusal Feature Extraction

The refusal feature reflects the model’s ability to distinguish between harmful and harmless prompts and to generate refusal responses only for harmful inputs. Therefore, it is most effective to extract the refusal feature from a layer that maximizes the distinction between harmful and harmless prompt representations. Based on a prior work [23] suggesting that such layers are typically located in the early to middle layers of LLMs, we identify the optimal layer by evaluating classification accuracy and the norm difference between the average features of harmful and harmless prompts across 8 different layers. As shown in Table 9, both the classification accuracy and norm differences vary across layers. For each layer, the classification threshold is optimized to maximize classification performance. As a result, we used  $l = 11$  for the Gemma2-9B [42] model and  $l = 18$  for the Qwen2-7B model in all of our experiments. For Llama3-7B, we adopted  $l = 12$ , following a prior work [3]. Additionally, we used the feature corresponding to the last input token, as it encodes the entire sentence due to the language model’s causal structure and attention masking.

### B.2 Effect of Cycle Length on Refusal Feature Updates

During the teacher preparation stage, the cycle determines both the interval and the number of samples used to update the standard refusal feature, which serves as important reference for distinguishing between features of harmful and harmless prompts in our ReFT model. A short cycle updates the standard refusal feature more frequently but with fewer samples, which can lead to unstable training due to variance of refusal features. In contrast, a long cycle uses more samples for each update but, due to its infrequent updates, may overfit to suboptimal refusal features. Table 10 presents the harmful score and finetuning accuracy across different cycle lengths and the corresponding number of samples used for updating the standard refusal feature. The results show that frequent updates with a short cycle help the ReFT model more effectively separate harmful from harmless prompts and generate appropriate refusal responses to harmful inputs.

Table 9: Classification accuracy and feature norm differences across layers for identifying the optimal layer index used to extract refusal features in Gemma2-9B-it and Qwen2-7B-Instruct. The selected layer used in our experiments is highlighted in bold. For each layer, features are extracted from the last input token.

(a) Gemma2-9B-it

| Layer idx | Threshold     | Harmful Acc (%) | Harmless Acc (%) | Acc (%)     | Harmful Avg   | Harmless Avg   | Diff          |
|-----------|---------------|-----------------|------------------|-------------|---------------|----------------|---------------|
| 7         | 0.0055        | 76.6            | 93.4             | 85.0        | 0.0239        | -0.0090        | 0.0329        |
| 8         | 0.0225        | 69.8            | 93.8             | 81.8        | 0.0374        | 0.0080         | 0.0294        |
| 9         | 0.0510        | 89.6            | 96.6             | 93.1        | 0.0878        | 0.0303         | 0.0575        |
| 10        | 0.0530        | 93.8            | 95.0             | 94.4        | 0.0949        | 0.0363         | 0.0586        |
| <b>11</b> | <b>0.0245</b> | <b>96.2</b>     | <b>98.6</b>      | <b>97.4</b> | <b>0.0844</b> | <b>-0.0020</b> | <b>0.0864</b> |
| 12        | 0.0555        | 91.4            | 96.4             | 93.9        | 0.1133        | 0.0319         | 0.0814        |
| 13        | 0.0570        | 90.8            | 92.8             | 91.8        | 0.1285        | 0.0346         | 0.0939        |
| 14        | 0.184         | 86.6            | 91.2             | 88.9        | 0.2629        | 0.1524         | 0.01105       |

(b) Qwen2-7B-Instruct

| Layer idx | Threshold    | Harmful Acc (%) | Harmless Acc (%) | Acc (%)     | Harmful Avg   | Harmless Avg  | Diff          |
|-----------|--------------|-----------------|------------------|-------------|---------------|---------------|---------------|
| 13        | 0.046        | 96.4            | 98.6             | 97.5        | 0.1814        | 0.0153        | 0.1661        |
| 14        | 0.118        | 97.2            | 97.8             | 97.5        | 0.2622        | 0.0875        | 0.1747        |
| 15        | 0.060        | 98.0            | 98.2             | 98.1        | 0.2297        | 0.0265        | 0.2032        |
| 16        | 0.145        | 96.2            | 99.2             | 97.7        | 0.3003        | 0.1093        | 0.1910        |
| 17        | 0.164        | 98.6            | 97.8             | 98.2        | 0.3709        | 0.1326        | 0.2383        |
| <b>18</b> | <b>0.195</b> | <b>98.6</b>     | <b>99.8</b>      | <b>99.2</b> | <b>0.4166</b> | <b>0.1551</b> | <b>0.2615</b> |
| 19        | 0.163        | 97.4            | 99.6             | 98.5        | 0.3555        | 0.1262        | 0.2293        |
| 20        | 0.055        | 95.0            | 99.4             | 97.2        | 0.2458        | 0.0211        | 0.2247        |

Table 10: Effect of cycle length (C) on the ReFT model performance.

| Cycle    | $N_{us} = N_s$ | HS ( $\downarrow$ ) | FA ( $\uparrow$ ) |
|----------|----------------|---------------------|-------------------|
| <b>6</b> | <b>30</b>      | <b>0.5</b>          | <b>49.0</b>       |
| 20       | 100            | 1.1                 | 47.8              |
| 100      | 500            | 1.1                 | 47.7              |
| 200      | 1000           | 1.2                 | 46.8              |

Table 11: Varying Lambda.

| $\lambda$  | HS ( $\downarrow$ ) | FA ( $\uparrow$ ) |
|------------|---------------------|-------------------|
| 0.05       | 0.7                 | 48.4              |
| <b>0.1</b> | <b>0.5</b>          | <b>49.0</b>       |
| 0.3        | 1.0                 | 48.3              |
| 0.5        | 1.0                 | 48.3              |
| 1.0        | 1.6                 | 47.7              |

Table 12: Varying Threshold.

| Threshold  | HS ( $\downarrow$ ) | FA ( $\uparrow$ ) |
|------------|---------------------|-------------------|
| 0          | 0.9                 | 47.8              |
| 0.3        | 0.6                 | 46.2              |
| 0.5        | 1.4                 | 47.2              |
| 0.7        | 1.0                 | 47.1              |
| <b>0.9</b> | <b>0.5</b>          | <b>49.0</b>       |

### B.3 Effect of Regularization Strength ( $\lambda$ ) on ReFT Model Training

The lambda value in Eq.1 of main manuscript controls the strength of the regularization term that encourages distinct separation between the features of harmful and harmless prompts in the ReFT model during the teacher preparation stage. An overly strong regularization term may disrupt the internal representations of the ReFT model, while a weak regularization term may reduce the ReFT model’s ability to distinguish between harmful and harmless prompts based on its refusal feature. Therefore, selecting an appropriate lambda value is critical for effective training of the ReFT model and subsequent finetuning. Table 11 presents the finetuning performance using ReFT models trained with different lambda values. The results show that a lambda value of 0.1 achieves the lowest harmful score and the highest finetuning accuracy, indicating its effectiveness as an optimal hyperparameter choice.

### B.4 Effect of Threshold Values on Finetuning

The threshold is a key hyperparameter used as a standard to classify harmful prompts by measuring the similarity between input prompt features and refusal features in the ReFT model during the finetuning stage. We predicted prompts with similarity above the threshold as harmful, while those below the threshold are classified as harmless. Therefore, a threshold that is too low may misclassify harmful prompts as harmless, thereby introducing safety risks by allowing harmful prompts to be included in finetuning. Conversely, a threshold that is too high may incorrectly filter out harmless prompts misclassified as harmful, leading to reduced finetuning accuracy. As shown in Table 12, we evaluate the impact of varying threshold values. The results indicate that a threshold of 0.9 yields the lowest harmful score and the highest finetuning accuracy. This optimal performance is attributed

Table 13: Impact of temperature ( $T$ ) and distillation weight ( $\alpha$ ) on Harmful Score (HS) and Finetuning Accuracy (FA). The best-performing setting ( $T = 1.0$ ,  $\alpha = 0.1$ ) is highlighted in bold.

| Temperature $T$ | $\alpha$   | HS ( $\downarrow$ ) | FA ( $\uparrow$ ) |
|-----------------|------------|---------------------|-------------------|
| <b>1.0</b>      | <b>0.1</b> | <b>0.5</b>          | <b>49.0</b>       |
| 1.0             | 0.3        | 1.3                 | 45.3              |
| 1.0             | 0.5        | 1.2                 | 47.9              |
| 1.0             | 1.0        | 1.2                 | 44.6              |
| 1.0             | 5.0        | 0.9                 | 40.5              |
| 2.0             | 0.1        | 0.9                 | 45.6              |
| 2.0             | 0.3        | 0.7                 | 44.2              |
| 2.0             | 0.5        | 1.0                 | 43.4              |
| 2.0             | 1.0        | 0.5                 | 42.8              |
| 2.0             | 5.0        | 0.6                 | 26.1              |
| 5.0             | 0.1        | 12.8                | 46.7              |
| 5.0             | 0.3        | 3.4                 | 46.5              |
| 5.0             | 0.5        | 3.1                 | 45.2              |
| 5.0             | 1.0        | 2.2                 | 44.2              |
| 5.0             | 5.0        | 2.4                 | 33.7              |

Table 14: Performance comparison of aligned LLMs used as ReFT models compared to their zero-shot performance. Using aligned LLMs as ReFT models improves both safety and task performance, though gains vary depending on the model.

| Aligned Model                  | HS ( $\downarrow$ ) | FA ( $\uparrow$ ) |
|--------------------------------|---------------------|-------------------|
| Llama3-8B (zero-shot)          | 74.6                | 14.2              |
| LlamaGuard3 (ReFT)             | 7.4                 | 49.5              |
| Llama3-8B-Instruct (zero-shot) | 18.7                | 60.7              |
| Llama3-8B-Instruct (ReFT)      | 13.9                | 65.8              |
| Gemma2-9B-it (zero-shot)       | 5.9                 | 74.3              |
| Gemma2-9B-it (ReFT)            | 4.9                 | 72.4              |
| Qwen2-7B-Instruct (zero-shot)  | 22.8                | 33.9              |
| Qwen2-7B-Instruct (ReFT)       | 20.6                | 73.2              |

to the near-perfect alignment of harmful prompt features with the refusal feature, resulting in the similarity values close to 1, in the ReFT model, as illustrated in Fig. 1 of the main manuscript.

## B.5 Effect of Distillation Hyperparameters

Knowledge distillation typically involves two key hyperparameters: temperature  $T$ , which controls the softness of the teacher predictions, and the distillation weight  $\alpha$ , which balances the influence of the distillation loss. To evaluate their impact, we measure both the harmful score and finetuning accuracy across various values of  $T$  and  $\alpha$ . As shown in Table 13, higher values of  $T$  lead to increased harmful scores, likely due to the student model not closely following the ReFT model’s predictions. In contrast, higher values of  $\alpha$  reduce the harmful score but also lower the finetuning accuracy, as excessive emphasis on the alignment loss weakens user-specific downstream task performance. Among these hyperparameter values,  $T = 1$  and  $\alpha = 0.1$  yield the best overall performance. This setting allows the student model to closely follow the well-aligned refusal responses of the ReFT model, while keeping the alignment loss moderate to preserve downstream task performance.

## C Additional Experiments

### C.1 Using Aligned LLMs as ReFT Models

Our settings assume that aligned LLMs are unavailable, and thus we train the ReFT model independently during teacher preparation stage. However, in real-world scenarios, many aligned models already exist, such as Llama3-8B-Instruct [2], Gemma2-9B-it [42], and Qwen2-7B-Instruct [1]. To evaluate the potential of using aligned LLMs as the ReFT model, we measure harmful scores and finetuning accuracy when using the aligned LLMs both as the ReFT model and as the base model. As a result, Table 14 shows that aligned LLMs can support classifying harmful prompts and distilling alignment knowledge, resulting in improvements in both harmful score and finetuning accuracy



Table 15: Performance comparison across different jailbreak attacks during finetuning. The GCG attack is generated using 100 samples from the BeaverTails dataset [19], and the AutoDAN attack is generated using 520 samples from the AdvBench dataset [55]. The results demonstrate the strong safety alignment and generalization capability of our ReFT-based finetuning strategy, which consistently outperforms all baselines.

| Methods       | BeaverTails [19] |             | GCG [55]   |             | AutoDAN [27] |             | Average    |             |
|---------------|------------------|-------------|------------|-------------|--------------|-------------|------------|-------------|
|               | HS ↓             | FA ↑        | HS ↓       | FA ↑        | HS ↓         | FA ↑        | HS ↓       | FA ↑        |
| SFT           | 16.7             | 40.6        | 36.0       | 40.6        | 69.6         | 40.6        | 40.8       | 40.6        |
| Repnoise [36] | 30.4             | 38.4        | 46.0       | 38.4        | 68.5         | 38.4        | 48.3       | 38.4        |
| Vaccine [16]  | 4.8              | 24.4        | 16.0       | 24.4        | 18.3         | 24.4        | 10.4       | 24.4        |
| Booster [15]  | 5.9              | 43.4        | 10.0       | 43.4        | 37.1         | 43.4        | 17.7       | 43.4        |
| LDIFS [30]    | 4.0              | 17.0        | <b>4.0</b> | 17.0        | 61.9         | 17.0        | 23.3       | 17.0        |
| Lisa [14]     | 5.3              | 38.3        | 52.0       | 38.3        | 41.5         | 38.3        | 32.9       | 38.3        |
| ReFT (Ours)   | <b>0.5</b>       | <b>49.0</b> | 6.0        | <b>49.0</b> | <b>0.9</b>   | <b>49.0</b> | <b>2.5</b> | <b>49.0</b> |

compared to their zero-shot performance. Nevertheless, their suboptimal classification accuracy limits the performance enhancement. In addition, Table 14 indicates that LlamaGuard3 [28], a model specifically designed to classify harmful and harmless prompts, can also be used as a ReFT model. For this experiment, Llama3-8B is used as the base model. These findings highlight both the practical feasibility of using existing aligned models as the ReFT model and the importance of a separate teacher preparation stage for maximizing classification performance.

## C.2 Robustness against Advanced Jailbreaking Attack

When jailbreaking LLMs, advanced techniques such as GCG (Greedy Coordinate Gradient)<sup>1</sup> [55] and AutoDAN (Automatically generating DAN-series-like jailbreak prompts)<sup>2</sup> [27] can be used to induce harmful responses beyond simply prompting with harmful queries. These methods demonstrated a high attack success rate in eliciting harmful responses, even from aligned models, compared to direct harmful prompts. To evaluate the robustness of our ReFT-based finetuning strategy against such advanced jailbreaking attacks, we measure harmful score under both GCG and AutoDAN attacks, targeting Llama3-8B-Instruct in a black-box setting. While all methods show increased harmful scores under these advanced attacks, Table 15 demonstrates that our ReFT-based finetuning method is more robust than baseline approaches. Notably, although the LDIFS method achieves a low harmful score under the GCG attack, it suffers from poor finetuning accuracy and exhibits a high harmful score under the AutoDAN attack, supporting its impracticality. In contrast, our method maintains both a low harmful score and high finetuning accuracy under both GCG and AutoDAN attacks, demonstrating its effectiveness in providing reliable protection against increasingly sophisticated jailbreak attempts.

## D Additional Analysis on Finetuning Datasets

We conduct additional analyses on GSM8K [7], SST2 [39], and AGNEWS [51] datasets, which are used during the finetuning stage. Similar to Fig. 1 and Table 1 in the main manuscript, we used BeaverTails [19] as the harmful data and GSM8K, SST2, and AGNEWS as the harmless data, and employed Llama3-8B [2] as the model architecture. Figure 2 illustrates the similarity distributions between input prompt features and the refusal feature, while Table 16 reports the classification accuracy for each dataset using its corresponding optimal threshold. Unlike Alpaca dataset [41], which contains general-purpose prompts, the downstream task datasets (GSM8K, SST2, AGNEWS) consist of domain-specific prompts and therefore differ in data distribution from BeaverTails. As a result, these datasets are slightly distinguishable even in the base model. However, aligned models exhibit more distinct similarity distributions and higher classification accuracy, while the ReFT model achieves the clearest separation and the highest classification performance. These results, consistent with Fig. 1 and Table 1 in the main manuscript, further support the generalization and reliability of our analysis.

<sup>1</sup><https://github.com/GraySwanAI/nanoGCG>

<sup>2</sup><https://github.com/SheltonLiu-N/AutoDAN>

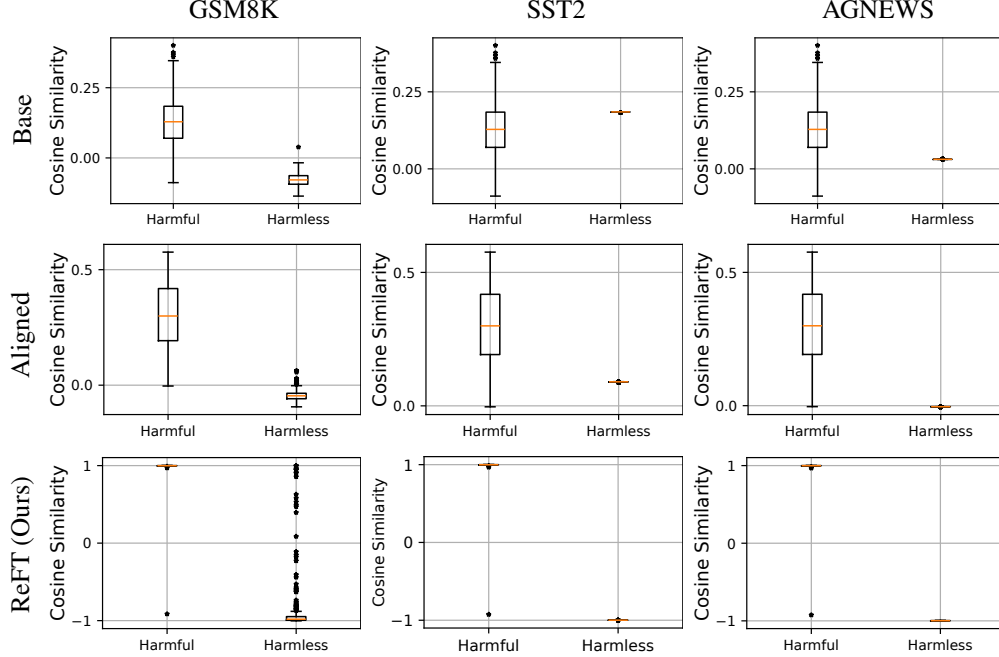


Figure 2: Box plot of cosine similarity distributions for harmful and harmless prompts, evaluated on the base model, aligned model, and ReFT (Ours). Harmful prompts were sampled from the BeaverTails dataset ( $n = 500$ ), while harmless prompts were sampled from GSM8K, SST2, and AGNEWS ( $n = 500$ ), which are domain-specific downstream task datasets used during the finetuning stage.

Table 16: Classification accuracy using refusal features. Prompts with cosine similarity above the threshold are identified as harmful, and those below as harmless. Thresholds are optimized to maximize total classification accuracy.

| Datasets | Model              | Threshold | Harmful Acc | Harmless Acc | Total Acc |
|----------|--------------------|-----------|-------------|--------------|-----------|
| GSM8K    | Llama3-8B          | -0.017    | 95.6%       | 99.8%        | 97.7%     |
|          | Llama3-8B-Instruct | 0.035     | 98.2%       | 99.6%        | 98.9%     |
|          | Llama3-8B-ReFT     | 0.965     | 99.8%       | 99.2%        | 99.5%     |
| SST2     | Llama3-8B          | 0.190     | 22.6%       | 100.0%       | 61.3%     |
|          | Llama3-8B-Instruct | 0.095     | 89.6%       | 100.0%       | 94.8%     |
|          | Llama3-8B-ReFT     | -0.920    | 100.0%      | 100.0%       | 100.0%    |
| AGNEWS   | Llama3-8B          | 0.032     | 86.0%       | 100.0%       | 93.0%     |
|          | Llama3-8B-Instruct | 0.010     | 99.8%       | 100.0%       | 99.9%     |
|          | Llama3-8B-ReFT     | -0.990    | 100.0%      | 100.0%       | 100.0%    |

## References

- [1] Qwen2 technical report. 2024.
- [2] AI@Meta. Llama 3 model card. 2024.
- [3] Andy Ardit, Oscar Obeso, Aaqib Syed, Daniel Paleka, Nina Panickssery, Wes Gurnee, and Neel Nanda. Refusal in language models is mediated by a single direction. *arXiv preprint arXiv:2406.11717*, 2024.
- [4] Somnath Banerjee, Sayan Layek, Soham Tripathy, Shanu Kumar, Animesh Mukherjee, and Rima Hazra. Safeinfer: Context adaptive decoding time safety alignment for large language models. In *Proceedings of the AAAI Conference on Artificial Intelligence*, volume 39, pages 27188–27196, 2025.
- [5] Federico Bianchi, Mirac Suzgun, Giuseppe Attanasio, Paul Röttger, Dan Jurafsky, Tatsunori Hashimoto, and James Zou. Safety-tuned llamas: Lessons from improving the safety of large language models that follow instructions. *arXiv preprint arXiv:2309.07875*, 2023.

- [6] Patrick Chao, Alexander Robey, Edgar Dobriban, Hamed Hassani, George J Pappas, and Eric Wong. Jailbreaking black box large language models in twenty queries. *arXiv preprint arXiv:2310.08419*, 2023.
- [7] Karl Cobbe, Vineet Kosaraju, Mohammad Bavarian, Mark Chen, Heewoo Jun, Lukasz Kaiser, Matthias Plappert, Jerry Tworek, Jacob Hilton, Reiichiro Nakano, Christopher Hesse, and John Schulman. Training verifiers to solve math word problems. *arXiv preprint arXiv:2110.14168*, 2021.
- [8] Yanrui Du, Sendong Zhao, Danyang Zhao, Ming Ma, Yuhan Chen, Liangyu Huo, Qing Yang, Dongliang Xu, and Bing Qin. Mogu: A framework for enhancing safety of open-sourced llms while preserving their usability. *arXiv preprint arXiv:2405.14488*, 2024.
- [9] Daya Guo, Dejian Yang, Haowei Zhang, Junxiao Song, Ruoyu Zhang, Runxin Xu, Qihao Zhu, Shiron Ma, Peiyi Wang, Xiao Bi, et al. Deepseek-r1: Incentivizing reasoning capability in llms via reinforcement learning. *arXiv preprint arXiv:2501.12948*, 2025.
- [10] Chia-Yi Hsu, Yu-Lin Tsai, Chih-Hsun Lin, Pin-Yu Chen, Chia-Mu Yu, and Chun-Ying Huang. Safe lora: The silver lining of reducing safety risks when finetuning large language models. *Advances in Neural Information Processing Systems*, 37:65072–65094, 2024.
- [11] Edward J Hu, Yelong Shen, Phillip Wallis, Zeyuan Allen-Zhu, Yuanzhi Li, Shean Wang, Lu Wang, Weizhu Chen, et al. Lora: Low-rank adaptation of large language models. *ICLR*, 1(2):3, 2022.
- [12] Xiaomeng Hu, Pin-Yu Chen, and Tsung-Yi Ho. Gradient cuff: Detecting jailbreak attacks on large language models by exploring refusal loss landscapes. *arXiv preprint arXiv:2403.00867*, 2024.
- [13] Tiansheng Huang, Gautam Bhattacharya, Pratik Joshi, Josh Kimball, and Ling Liu. Antidote: Post-fine-tuning safety alignment for large language models against harmful fine-tuning. *arXiv preprint arXiv:2408.09600*, 2024.
- [14] Tiansheng Huang, Sihao Hu, Fatih Ilhan, Selim Tekin, and Ling Liu. Lisa: Lazy safety alignment for large language models against harmful fine-tuning attack. *Advances in Neural Information Processing Systems*, 37:104521–104555, 2024.
- [15] Tiansheng Huang, Sihao Hu, Fatih Ilhan, Selim Furkan Tekin, and Ling Liu. Booster: Tackling harmful fine-tuning for large language models via attenuating harmful perturbation. *arXiv preprint arXiv:2409.01586*, 2024.
- [16] Tiansheng Huang, Sihao Hu, and Ling Liu. Vaccine: Perturbation-aware alignment for large language models against harmful fine-tuning attack. *arXiv preprint arXiv:2402.01109*, 2024.
- [17] Kuo-Han Hung, Ching-Yun Ko, Ambrish Rawat, I Chung, Winston H Hsu, Pin-Yu Chen, et al. Attention tracker: Detecting prompt injection attacks in llms. *arXiv preprint arXiv:2411.00348*, 2024.
- [18] Aaron Hurst, Adam Lerer, Adam P Goucher, Adam Perelman, Aditya Ramesh, Aidan Clark, AJ Ostrow, Akila Welihinda, Alan Hayes, Alec Radford, et al. Gpt-4o system card. *arXiv preprint arXiv:2410.21276*, 2024.
- [19] Jiaming Ji, Mickel Liu, Josef Dai, Xuehai Pan, Chi Zhang, Ce Bian, Boyuan Chen, Ruiyang Sun, Yizhou Wang, and Yaodong Yang. Beavertails: Towards improved safety alignment of llm via a human-preference dataset. *Advances in Neural Information Processing Systems*, 36:24678–24704, 2023.
- [20] Albert Qiaochu Jiang, Alexandre Sablayrolles, Arthur Mensch, Chris Bamford, Devendra Singh Chaplot, Diego de Las Casas, Florian Bressand, Gianna Lengyel, Guillaume Lample, Lucile Saulnier, L’elio Renard Lavaud, Marie-Anne Lachaux, Pierre Stock, Teven Le Scao, Thibaut Lavril, Thomas Wang, Timothée Lacroix, and William El Sayed. Mistral 7b. *ArXiv*, abs/2310.06825, 2023.

- [21] Simon Lermen, Charlie Rogers-Smith, and Jeffrey Ladish. Lora fine-tuning efficiently undoes safety training in llama 2-chat 70b. *arXiv preprint arXiv:2310.20624*, 2023.
- [22] Mingjie Li, Wai Man Si, Michael Backes, Yang Zhang, and Yisen Wang. Salora: Safety-alignment preserved low-rank adaptation. *arXiv preprint arXiv:2501.01765*, 2025.
- [23] Shen Li, Liuyi Yao, Lan Zhang, and Yaliang Li. Safety layers in aligned large language models: The key to llm security. *arXiv preprint arXiv:2408.17003*, 2024.
- [24] Xiao Li, Zhuhong Li, Qiongxiu Li, Bingze Lee, Jinghao Cui, and Xiaolin Hu. Faster-gcg: Efficient discrete optimization jailbreak attacks against aligned large language models. *arXiv preprint arXiv:2410.15362*, 2024.
- [25] Xuechen Li, Tianyi Zhang, Yann Dubois, Rohan Taori, Ishaan Gulrajani, Carlos Guestrin, Percy Liang, and Tatsunori B. Hashimoto. AlpacaEval: An automatic evaluator of instruction-following models. [https://github.com/tatsu-lab/alpaca\\_eval](https://github.com/tatsu-lab/alpaca_eval), 5 2023.
- [26] Guozhi Liu, Weiwei Lin, Tiansheng Huang, Ruichao Mo, Qi Mu, and Li Shen. Targeted vaccine: Safety alignment for large language models against harmful fine-tuning via layer-wise perturbation. *arXiv preprint arXiv:2410.09760*, 2024.
- [27] Xiaogeng Liu, Nan Xu, Muhao Chen, and Chaowei Xiao. Autodan: Generating stealthy jailbreak prompts on aligned large language models. *arXiv preprint arXiv:2310.04451*, 2023.
- [28] AI @ Meta Llama Team. The llama 3 herd of models, 2024.
- [29] Ilya Loshchilov and Frank Hutter. Decoupled weight decay regularization. *arXiv preprint arXiv:1711.05101*, 2017.
- [30] Jishnu Mukhoti, Yarin Gal, Philip HS Torr, and Puneet K Dokania. Fine-tuning can cripple your foundation model; preserving features may be the solution. *arXiv preprint arXiv:2308.13320*, 2023.
- [31] Long Ouyang, Jeffrey Wu, Xu Jiang, Diogo Almeida, Carroll Wainwright, Pamela Mishkin, Chong Zhang, Sandhini Agarwal, Katarina Slama, Alex Ray, et al. Training language models to follow instructions with human feedback. *Advances in neural information processing systems*, 35:27730–27744, 2022.
- [32] et al. Qi. Constrain-sft: A supervised fine-tuning approach to enhance safety alignment in large language models. *Proceedings of NeurIPS 2024*, 37:95174, 2024.
- [33] Xiangyu Qi, Yi Zeng, Tinghao Xie, Pin-Yu Chen, Ruoxi Jia, Prateek Mittal, and Peter Henderson. Fine-tuning aligned language models compromises safety, even when users do not intend to! *arXiv preprint arXiv:2310.03693*, 2023.
- [34] Rafael Rafailov, Archit Sharma, Eric Mitchell, Christopher D Manning, Stefano Ermon, and Chelsea Finn. Direct preference optimization: Your language model is secretly a reward model. *Advances in Neural Information Processing Systems*, 36:53728–53741, 2023.
- [35] LG Research, Kyunghoon Bae, Eunbi Choi, Kibong Choi, Stanley Jungkyu Choi, Yemuk Choi, Seokhee Hong, Junwon Hwang, Hyojin Jeon, Kijeong Jeon, et al. Exaone deep: Reasoning enhanced language models. *arXiv preprint arXiv:2503.12524*, 2025.
- [36] Domenic Rosati, Jan Wehner, Kai Williams, Lukasz Bartoszcze, Robie Gonzales, Subhabrata Majumdar, Hassan Sajjad, Frank Rudzicz, et al. Representation noising: A defence mechanism against harmful finetuning. *Advances in Neural Information Processing Systems*, 37:12636–12676, 2024.
- [37] Abhay Sheshadri, Aidan Ewart, Phillip Guo, Aengus Lynch, Cindy Wu, Vivek Hebbar, Henry Sleight, Asa Cooper Stickland, Ethan Perez, Dylan Hadfield-Menell, et al. Targeted latent adversarial training improves robustness to persistent harmful behaviors in llms. *arXiv e-prints*, pages arXiv–2407, 2024.

- [38] Abhay Sheshadri, Aidan Ewart, Phillip Guo, Aengus Lynch, Cindy Wu, Vivek Hebbar, Henry Sleight, Asa Cooper Stickland, Ethan Perez, Dylan Hadfield-Menell, et al. Latent adversarial training improves robustness to persistent harmful behaviors in llms. *arXiv preprint arXiv:2407.15549*, 2024.
- [39] Richard Socher, Alex Perelygin, Jean Wu, Jason Chuang, Christopher D. Manning, Andrew Ng, and Christopher Potts. Recursive deep models for semantic compositionality over a sentiment treebank. In *Proceedings of the 2013 Conference on Empirical Methods in Natural Language Processing*, pages 1631–1642, Seattle, Washington, USA, October 2013. Association for Computational Linguistics.
- [40] Rishub Tamirisa, Bhrugu Bharathi, Long Phan, Andy Zhou, Alice Gatti, Tarun Suresh, Maxwell Lin, Justin Wang, Rowan Wang, Ron Arel, et al. Tamper-resistant safeguards for open-weight llms. *arXiv preprint arXiv:2408.00761*, 2024.
- [41] Rohan Taori, Ishaan Gulrajani, Tianyi Zhang, Yann Dubois, Xuechen Li, Carlos Guestrin, Percy Liang, and Tatsunori B. Hashimoto. Stanford alpaca: An instruction-following llama model. [https://github.com/tatsu-lab/stanford\\_alpaca](https://github.com/tatsu-lab/stanford_alpaca), 2023.
- [42] Gemma Team, Morgane Riviere, Shreya Pathak, Pier Giuseppe Sessa, Cassidy Hardin, Surya Bhupatiraju, Léonard Hussenot, Thomas Mesnard, Bobak Shahriari, Alexandre Ramé, et al. Gemma 2: Improving open language models at a practical size. *arXiv preprint arXiv:2408.00118*, 2024.
- [43] Hugo Touvron, Thibaut Lavril, Gautier Izacard, Xavier Martinet, Marie-Anne Lachaux, Timothée Lacroix, Baptiste Rozière, Naman Goyal, Eric Hambro, Faisal Azhar, et al. Llama: Open and efficient foundation language models. *arXiv preprint arXiv:2302.13971*, 2023.
- [44] Xunguang Wang, Daoyuan Wu, Zhenlan Ji, Zongjie Li, Pingchuan Ma, Shuai Wang, Yingjiu Li, Yang Liu, Ning Liu, and Juergen Rahmel. Selfdefend: Llms can defend themselves against jailbreaking in a practical manner. *arXiv preprint arXiv:2406.05498*, 2024.
- [45] et al. Wei. Freeze: A method to preserve safety alignment during fine-tuning of large language models. *Proceedings of NeurIPS 2024*, 37:96357, 2024.
- [46] Sophie Xhonneux, Alessandro Sordoni, Stephan Günnemann, Gauthier Gidel, and Leo Schwinn. Efficient adversarial training in llms with continuous attacks. *arXiv preprint arXiv:2405.15589*, 2024.
- [47] Yueqi Xie, Minghong Fang, Renjie Pi, and Neil Gong. Gradsafe: Detecting jailbreak prompts for llms via safety-critical gradient analysis. *arXiv preprint arXiv:2402.13494*, 2024.
- [48] Zhangchen Xu, Fengqing Jiang, Luyao Niu, Jinyuan Jia, Bill Yuchen Lin, and Radha Pooven-dran. Safedecoding: Defending against jailbreak attacks via safety-aware decoding. *arXiv preprint arXiv:2402.08983*, 2024.
- [49] Xin Yi, Shunfan Zheng, Linlin Wang, Gerard de Melo, Xiaoling Wang, and Liang He. Nlsr: Neuron-level safety realignment of large language models against harmful fine-tuning. In *Proceedings of the AAAI Conference on Artificial Intelligence*, volume 39, pages 25706–25714, 2025.
- [50] Lei Yu, Virginie Do, Karen Hambardzumyan, and Nicola Cancedda. Robust llm safeguarding via refusal feature adversarial training. *arXiv preprint arXiv:2409.20089*, 2024.
- [51] Xiang Zhang, Junbo Jake Zhao, and Yann LeCun. Character-level convolutional networks for text classification. In *NIPS*, 2015.
- [52] Yuqi Zhang, Liang Ding, Lefei Zhang, and Dacheng Tao. Intention analysis makes llms a good jailbreak defender. *arXiv preprint arXiv:2401.06561*, 2024.
- [53] Zhengyue Zhao, Xiaoyun Zhang, Kaidi Xu, Xing Hu, Rui Zhang, Zidong Du, Qi Guo, and Yunji Chen. Adversarial contrastive decoding: Boosting safety alignment of large language models via opposite prompt optimization. *arXiv preprint arXiv:2406.16743*, 2024.

- [54] Andy Zou, Long Phan, Justin Wang, Derek Duenas, Maxwell Lin, Maksym Andriushchenko, J Zico Kolter, Matt Fredrikson, and Dan Hendrycks. Improving alignment and robustness with circuit breakers. In *The Thirty-eighth Annual Conference on Neural Information Processing Systems*, 2024.
- [55] Andy Zou, Zifan Wang, J. Zico Kolter, and Matt Fredrikson. Universal and transferable adversarial attacks on aligned language models, 2023.